Appendix A

A1 Supplementary figures

Figure S1. Pearson correlation coefficients between mean seasonal rainfall over the Challa/Naivasha region and global SSTs in observations and climate models (here, only the first member r1i1p1 is used) for the period 1950-2000. In areas overprinted with white circles, a null hypothesis of no correlation can be rejected at the 5% level. No data are available from grey areas.

Figure S2. Same as in Fig. S1 but using rainfall averaged over the Masoko/Malawi region.

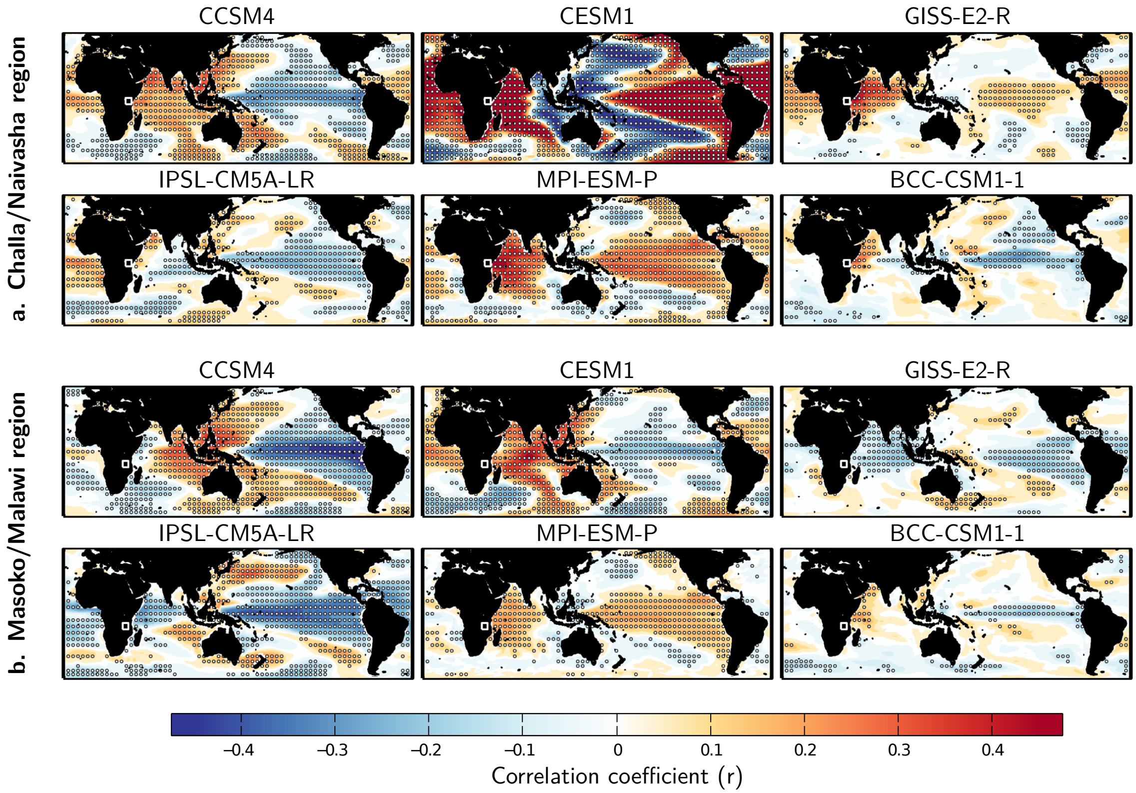

Figure S3. Pearson correlation coefficients between mean annual rainfall over the Challa/Naivasha region (a, upper two rows) or Masoko/Malawi region (b, lower two rows) and global SSTs in the *pre-industrial control* runs of the climate models. In areas overprinted with white circles, a null hypothesis of no correlation can be rejected at the 5% level. No data are available from grey areas.

A2 Supplementary tables

Table S1. Information about proxy-based reconstructions used in this study.

Site	Proxy type	Reconstructed variable	Period (yrs AD)	Mean temporal resolution (yrs)	Age model derived from	reference
Challa	Branched and isoprenoidal index (BIT)	Runoff	-22972–1980	124	^{14}C and ^{210}Pb	Verschuren et al. (2009)
Challa	δD_{wax}	Isotopic composition of rainfall	-22972–1980	180	^{14}C and ^{210}Pb	Tierney et al. (2011)
Challa	Varve thickness	Wind and rain-driven changes in lake biology	-1050–2005	1	Varve counts?	Wolff et al. (2011)
Naivasha	sediment stratigraphy, species compositions of fossil diatom and midge assemblages	Lake level	884–1993.6	3	^{14}C, ^{210}Pb and fossil evidence	(Verschuren et al., 2000)
Masoko	Low-field magnetic susceptibility	Wind-stress and/or lake-level amplitude changes	-43308–2001	25	^{14}C	Garcin et al. (2006)
Masoko	Low-field magnetic susceptibility	Wind-stress and/or lake-level amplitude changes	1511–2002	5	^{14}C, cross-core correlation, tephra	Garcin et al. (2007)
Malawi	Terrigenous mass accumulation rate (MAR)	Runoff	1270–1978	6	^{210}Pb and varves counts	Brown and Johnson (2005); Johnson and McCave (2008)

Table S2. Pearson correlation coefficients between observed and simulated rainfall-SSTs correlation maps for the Challa/Naivasha region (Fig. **??**a.) and the Masoko/Malawi region (Fig. **??**b.), for annual mean results and October-November-December (OND) mean results.

	Challa-Naivasha		**Masoko-Malawi**	
	annual	OND	annual	OND
CCSM4	-0.36*	-0.30*	0.07*	-0.26*
CESM1	0.27*	0.61*	-0.01	0.51*
GISS-E2-R	-0.01	-0.18*	0.24*	-0.16*
IPSL-CM5A-LR	-0.10*	-0.08*	0.10*	0.08*
MPI-ESM-P	0.16*	0.39*	0.15*	0.43*
BCC-CSM1-1	0.00	0.17*	0.05*	0.12*

* significant at the 5% level

Table S3. Pearson correlation coefficients between simulated and reconstructed hydroclimate time series. Model results over the region Challa/Naivasha (Masoko/Malawi) are compared to proxy-based reconstruction of Challa (Masoko), Naivasha (Malawi), and the mean between the two. The coefficients are computed over the periods covered by the data at annual resolution. Model time series are filtered using a loess method with a window of 100 years. The autocorrelation introduced in the model and reconstructions curves in response, respectively, to the smoothing and to the interpolation is taken into account when assessing the significance of the correlations (t-Test).

Variable: P–E	**Challa**	**Naivasha**	**Challa/Naivasha**	**Masoko**	**Malawi**	**Masoko/Malawi**
CCSM4	-0.03	0.22	-0.01	-0.03	0.12	-0.00
CESM1	-0.07	-0.16	-0.26	0.33	0.15	0.43*
GISS-E2-R	0.08	0.35	0.38*	-0.02	0.10	0.14
IPSL-CM5A-LR	0.01	-0.03	0.01	0.02	0.01	0.18
MPI-ESM-P	-0.05	-0.22	-0.23	-0.11	-0.13	-0.13
BCC-CSM1-1	0.26	-0.10	0.03	-0.28	-0.01	-0.03

* significant at the 5% level

A3 Supplementary discussion: comparison between reconstructions and the integration of simulated P-E

To address the issue concerning the memory mismatch between the simulated and the reconstructed hydroclimate variables, we have used a first order autoregressive model (AR-1) model driven by the simulated P-E time series, which introduces some memory in the system depending on the parameter α (Eq. A1):

$$X(t+1) = \alpha . X(t) + (P-E)(t) \tag{A1}$$

where X is the emulated system and α the autocorrelation parameter. Note that to be represented by an autoregressive model, the process has to be stochastic. Although P-E is not fully stochastic, it can be considered as not far to so this is not a strong violation of the assumption. All four sites have time scales of variability from a few decades to a century. We have thus chosen a similar α equal to 0.98, which means that 2% of the signal will be lost each year. We also have done the test with an α of 1, which represents the integration of the time series through the whole period. This is equivalent to the estimation of the level of a bucket with no runoff which is increasing if P-E is positive and decreasing if it is negative. This is an extreme case, since the long-term impact of any perturbation will be overestimated, but this provides useful upper bound to test the influence of the memory of the lake on model-data comparison. The AR-1 model with an α of 0.98 (Fig. S4) and the full integration of P-E (Fig. S5) emphasizes the low-frequency changes that lead time series to appear more similar to reconstructions.

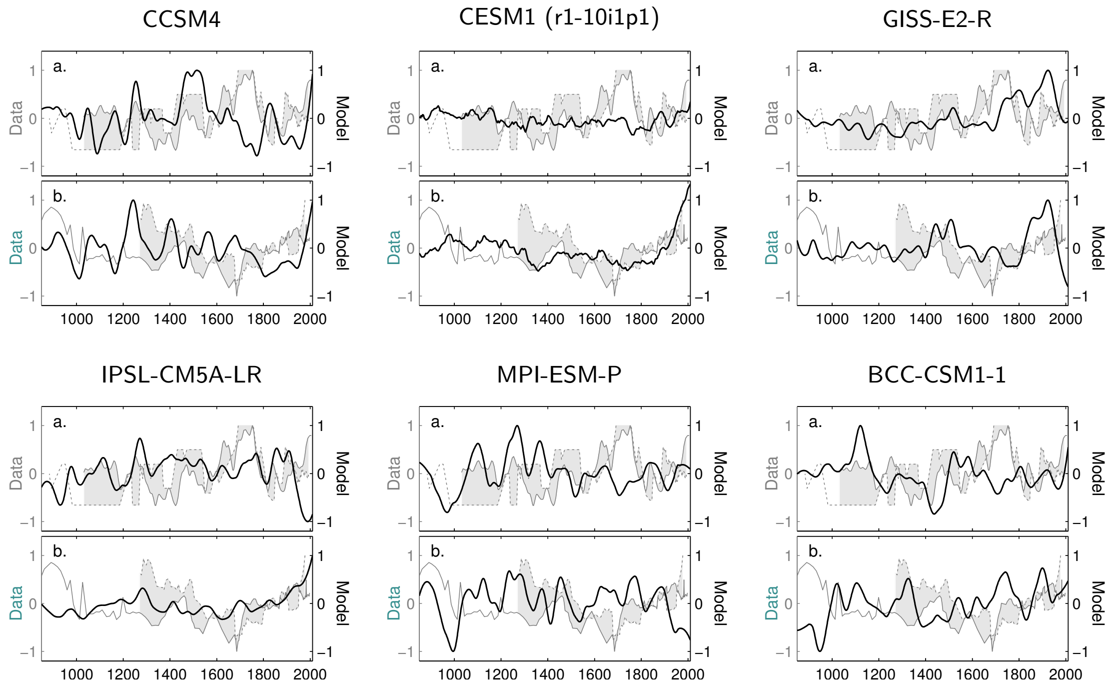

Figure S4. Comparison between last-millennium time series of the reconstructions (in grey) and of the AR1 model applied to P-E simulated by six GCMs (in black, using an α equal to 0.98) averaged over the Challa/Naivasha region (a), with the Naivasha record shown as dashed line and the Challa record as solid line; and over the Masoko/Malawi region (b), with the Malawi record shown as dashed line and the Masoko record as solid line. In both regions, the area between the between the two records is shaded in light grey. Both proxy-based and simulated time series are presented as anomalies with respect to the whole period, and are linearly standardized so that the absolute maximum equals 1. Ordinate axes are oriented such that wetter (drier) conditions point upwards (downwards). Model time series are annual mean values filtered using a loess method with a window of 100 years. For the CESM1 model, the black curve is the median of the ten ensemble members previously standardized and smoothed.

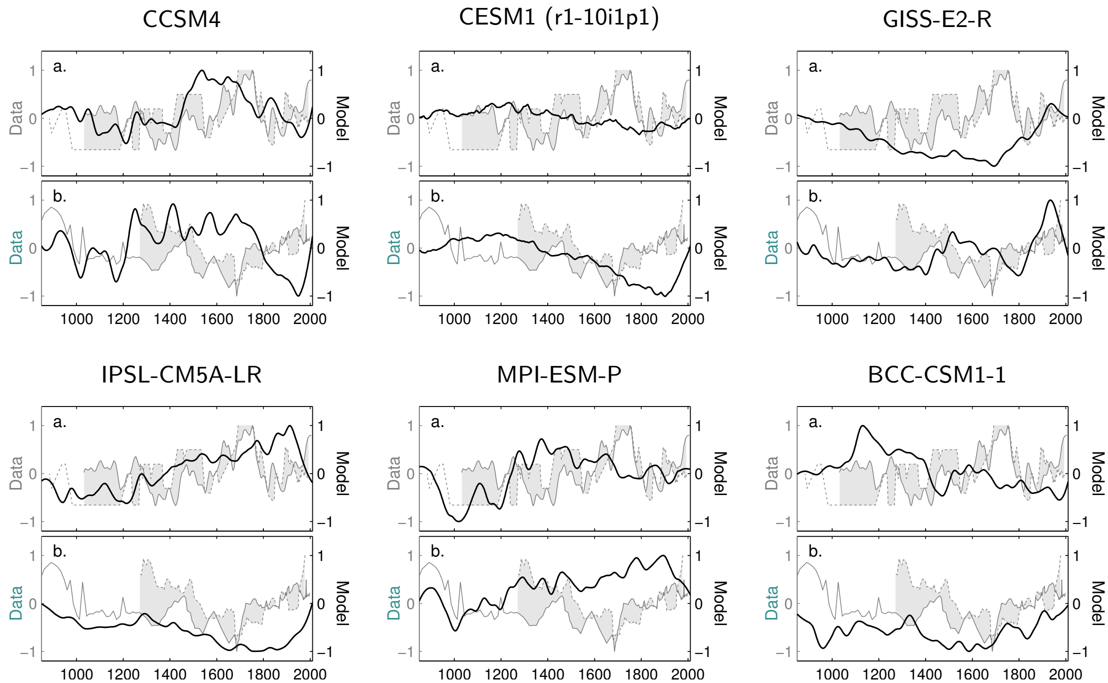

Figure S5. Same as in Fig. S4, but using the integration over the whole period of simulated P-E of models (AR1 model with an α of 1).

Although the absolute values of the correlation coefficients are generally higher, especially for the integrated time series (Tables S4 and S5), the model-data agreement is not substantially improved. Most models do not simulate any reconstructed time series, and the ones that show some skills at simulating reconstructed hydroclimate in one region perform badly in the other region. This is because, although they show different curves in Masoko/Malawi and in Challa/Naivasha they are unable to simulate the dipole between these regions as observed in reconstructions between 1400 to around 1800.

Table S4. Same as in Table S3, but using the AR1 model applied to the simulated time series of P-E in models, with α equal to 0.98.

Variable: P–E	**Challa**	**Naivasha**	**Challa/Naivasha**	**Masoko**	**Malawi**	**Masoko/Malawi**
CCSM4	-0.17	0.18	-0.12	-0.06	0.13	-0.13
CESM1	0.08	-0.37*	-0.24	0.29	0.29	0.43*
GISS-E2-R	0.05	0.33	0.27	0.11	0.11	0.31
IPSL-CM5A-LR	-0.18	0.14	0.08	0.11	0.30	0.52*
MPI-ESM-P	-0.14	-0.13	-0.38	-0.10	-0.04	-0.11
BCC-CSM1-1	0.07	-0.43*	-0.28	-0.32	-0.20	-0.06

* significant at the 5% level

Table S5. Same as in Table S3, but using the integration of simulated P-E in models over the whole period.

Variable: P–E	**Challa**	**Naivasha**	**Challa/Naivasha**	**Masoko**	**Malawi**	**Masoko/Malawi**
CCSM4	0.23	0.33	0.39*	-0.33	-0.10	-0.42
CESM1	-0.28	-0.35	-0.46*	-0.08	0.56*	0.14*
GISS-E2-R	0.02	-0.33	-0.28	0.22	-0.15	0.06
IPSL-CM5A-LR	0.14	0.52*	0.47*	0.42*	0.81*	0.60*
MPI-ESM-P	-0.18	0.56*	0.19	-0.06	-0.27	0.04
BCC-CSM1-1	-0.23	-0.54*	-0.52*	0.43*	0.30	0.55*

* significant at the 5% level

References

Brown, E. T. and Johnson, T. C.: Coherence between tropical East African and South American records of the Little Ice Age, Geochemistry, Geophysics, Geosystems, 6, 1–11, doi:10.1029/2005GC000959, 2005.

Garcin, Y., Williamson, D., Taieb, M., Vincens, A., Mathé, P. E., and Majule, A.: Centennial to millennial changes in maar-lake deposition during the last 45,000 years in tropical Southern Africa (Lake Masoko, Tanzania), Palaeogeography, Palaeoclimatology, Palaeoecology, 239, 334–354, doi:10.1016/j.palaeo.2006.02.002, 2006.

Garcin, Y., Williamson, D., Bergonzini, L., Radakovitch, O., Vincens, A., Buchet, G., Guiot, J., Brewer, S., Mathé, P. E., and Majule, A.: Solar and anthropogenic imprints on Lake Masoko (southern Tanzania) during the last 500 years, Journal of Paleolimnology, 37, 475–490, doi:10.1007/s10933-006-9033-6, 2007.

Johnson, T. C. and McCave, I. N.: Transport mechanism and paleoclimatic significance of terrigenous silt deposited in varved sediments of an African rift lake, Limnology and Oceanography, 53, 1622–1632, doi:10.4319/lo.2008.53.4.1622, 2008.

Tierney, J. E., Russell, J. M., Sinninghe Damsté, J. S., Huang, Y., and Verschuren, D.: Late Quaternary behavior of the East African monsoon and the importance of the Congo Air Boundary, Quaternary Science Reviews, 30, 798–807, doi:10.1016/j.quascirev.2011.01.017, http://linkinghub.elsevier.com/retrieve/pii/S0277379111000321, 2011.

Verschuren, D., Laird, K. R., and Cumming, B. F.: Rainfall and drought in equatorial east Africa during the past 1,100 years., Nature, 403, 410–414, doi:10.1038/35000179, 2000.

Verschuren, D., Sinninghe Damsté, J. S., Moernaut, J., Kristen, I., Blaauw, M., Fagot, M., and Haug, G. H.: Half-precessional dynamics of monsoon rainfall near the East African Equator., Nature, 462, 637–641, doi:10.1038/nature08520, http://dx.doi.org/10.1038/nature08520, 2009.

Wolff, C., Haug, G. H., Timmermann, A., Sinninghe Damsté, J. S., Brauer, A., Sigman, D. M., Cane, M. A., and Verschuren, D.: Reduced interannual rainfall variability in East Africa during the last ice age., Science (New York, N.Y.), 333, 743–747, doi:10.1126/science.1203724, 2011.